

Compressive Strength Evaluation of Concrete Confined With Spiral Stirrups by Using Adaptive Neuro-fuzzy Inference System (ANFIS)

Wei Chang (✉ changweihit@hit.edu.cn)

Harbin Institute of Technology

Wenzhong Zheng

Harbin Institute of Technology

Research Article

Keywords: Adaptive neural-fuzzy inference system (ANFIS), compressive strength, confined concrete, spiral stirrups, prediction model

Posted Date: December 1st, 2021

DOI: <https://doi.org/10.21203/rs.3.rs-1116845/v1>

License:   This work is licensed under a Creative Commons Attribution 4.0 International License.

[Read Full License](#)

Compressive strength evaluation of concrete confined with spiral stirrups by using adaptive neuro-fuzzy inference system (ANFIS)

Wei Chang^{3,*}, Wenzhong Zheng^{1,2,3}

¹ Key lab of Structures Dynamic Behavior and Control Ministry of Education, Harbin Institute of Technology, Harbin 150090, China

² Key Lab of Smart Prevention and Mitigation of Civil Engineering Disasters of the Ministry of Industry and Information Technology, Harbin Institute of Technology, Harbin, 150090, China

³ School of Civil Engineering, Harbin Institute of Technology, Harbin 150090, China

* Correspondence: School of Civil Engineering, Harbin Institute of Technology, 202 Haihe Road, Nangang District Harbin, China. E-mail: changweihit@hit.edu.cn

Abstract: The compressive strength of concrete confined with spiral stirrups was an important parameter to evaluate the load-bearing capacity of concrete columns. The confinement provided by spiral stirrups let concrete under the triaxial compression state and improved the compressive strength of concrete. However, the relationships between concrete and stirrups were complex and the existing prediction models for evaluating the compressive strength of confined concrete were various. In this paper, an adaptive neural-fuzzy inference system (ANFIS) model was developed to evaluate the compressive strength of concrete confined with stirrups. A set of 231 experimental results of concrete confined with spiral stirrups were collected from the previous studies to establish a reliable database. The investigated parameters included the aspect ratio of specimens, the diameter, spacing, yield strength, and volumetric ratio of stirrups, the ratio of longitudinal reinforcement, and the compressive strength of concrete. The results showed that the ANFIS model predicted the compressive strength of confined concrete accurately. By comparing with existing models, the proposed ANFIS model had high applicable and reliability. The effects of the investigated parameters on the compressive strength of concrete were analyzed based on the proposed ANFIS model.

Keywords: Adaptive neural-fuzzy inference system (ANFIS); compressive strength; confined concrete; spiral stirrups; prediction model

1. Introduction

The compressive strength of concrete was a crucial parameter to evaluate the load-bearing capacity of concrete columns. The compressive strength of concrete would be enhanced when concrete was confined with stirrups, which let concrete under triaxial compression [1]. It was important to evaluate the compressive strength of confined concrete. The compressive strength of confined concrete was close related to the mechanical properties of stirrups [2]. However, the relationships between concrete and stirrups were complex, which can be attributed to the tensile strength of stirrups may not reach the yield strength at the compressive strength of confined concrete [3]. It was not suitable for evaluating the compressive strength of confined concrete by using the tensile strength; on the other hand, the existing models for evaluating the compressive strength of confined concrete were proposed by the limited experimental data sets, which should be reevaluated when the new test data were introduced. Thus, it was necessary to establish a reliable prediction model to estimate the compressive strength of concrete confined with spiral stirrups.

The compression behavior of concrete confined with spiral stirrups has been studied over one century and many typical prediction models for evaluating the compressive strength of confined concrete were proposed. Richard et al. explored the compression behavior of confined concrete, and found that the compressive strength of confined concrete was improved by lateral confinement of

45 stirrups [4]. Besides, they firstly proposed the prediction models for evaluating the compressive
46 strength of confined concrete [5]. Mander et al. indicated that longitudinal reinforcement and spiral
47 stirrups both had obvious effects on the compressive strength of concrete based on the experimental
48 results and theoretical analysis [6] and the analytical model for predicting the compressive strength
49 of confined concrete by considering the effects of longitudinal reinforcement and stirrups based on
50 the "Mohr-Coulomb criteria"[7]. Cusson proposed the concept of "confinement index", which was
51 the ratio between the lateral confining stress and compressive stress of unconfined concrete, to
52 evaluate the compressive strength of confined concrete [8]. Legeron proposed a prediction model for
53 evaluating the compressive strength of confined concrete based on the theoretical analysis and a
54 large experimental results [3]. Bing found that the high strength of spiral stirrups can significantly
55 improve the compressive strength of confined concrete [9]. Saatcioglu and Razvi indicated that the
56 lateral confining stress decreased exponentially with the increase of concrete compressive strength
57 [10]. Sharma thought that the load-bearing capacity of confined concrete columns would be
58 decreased with the increase of the compressive strength of concrete, while the volumetric ratio and
59 spacing of stirrups had obvious influence on the compressive behavior of confined concrete [11].
60 Wang founded that the compressive strength of confined concrete increased with the increased of
61 the yield strength of stirrups, while the volumetric ratio of stirrups also had the same effects [12].
62 Wei demonstrated that the high strength steel wire can effectively improved the compressive
63 strength of confined concrete [13]. Cao found that the high strength stirrups had insignificant effects
64 on the load-bearing capacity of confined concrete [14]. Deng et al. found that high strength stirrups
65 had superiority in improving the compressive strength of confined concrete compared with normal
66 strength stirrups [15]. Based on the previous studies, the effects of the influential parameters on the
67 compressive strength of confined concrete only considered the yield strength and the volumetric
68 ratio of stirrups, and as well as the compressive strength of concrete. Moreover, the existing
69 prediction models were established based a specific set of experimental results, when new test
70 results were introduced, the applicability and reliability of models should be re-evaluated.
71 Moreover, some existing models with numerous variables and complex computational processes
72 were difficult to utilize in practical civil engineering design.

73 In recent years, adaptive neural-fuzzy inference system (ANFIS) combined with both learning
74 and reasoning capability of artificial neural network and fuzzy logic has been developed for solving
75 the complex problems [16]. Akbarpour proposed an ANFIS model to predict the punching shear
76 strength of two-way slabs based on 189 experimental results and found that the proposed model can
77 evaluate the punching load with an acceptable error [17]. Khademi [18] and Bilgehan [19] predicted
78 the 28 days compressive strength of recycled aggregate concrete by using ANFIS with 14 different
79 input parameters and indicated that the ANFIS model was suggested to be used in the mix design
80 optimization and be utilized for preliminary mix design of concrete, respectively. Vakhshouri
81 designed ANFIS models to establish the relationships between the compressive strength of
82 self-compacting concrete and mixture proportions and slump flow and indicated the proposed
83 models gave the best prediction of the compressive strength [20]. Based on the previous studies, the
84 ANFIS had high prediction performance and good reliable for predicting the mechanical properties
85 of concrete. Thus, ANFIS was suitable for evaluating the compressive strength of concrete confined
86 with stirrups.

87 The objective of this paper was to evaluate the compressive strength of concrete confined with
88 spiral stirrups. To achieve this purpose, 231-group experimental results of concrete confined with
89 spiral stirrups were collected from previous studies to establish a reliable database. Based on the
90 database, an ANFIS model was developed to evaluate the compressive strength of confined concrete.
91 Furthermore, the effects of the influential parameters on the compressive strength of confined
92 concrete were analyzed.

93 2. Database preparation

94 To establish the ANFIS model for evaluating the compressive strength of concrete confined
95 with spiral stirrups, a reliable database consisting of 231-group of experimental results of concrete

96 columns confined with spiral stirrups were gathered from the previous studies was established,
 97 listed in Table.5 attached in the appendix [6,22-37]. To ensure the reliable of the database, the
 98 collected data should obey the following criteria: (1) all specimens had one layer spiral stirrup; (2)
 99 the aspect ratio of all specimens was no more than 8 to avoid the bucking failure; (3) all specimens
 100 were tested under monotonically concentric loads.

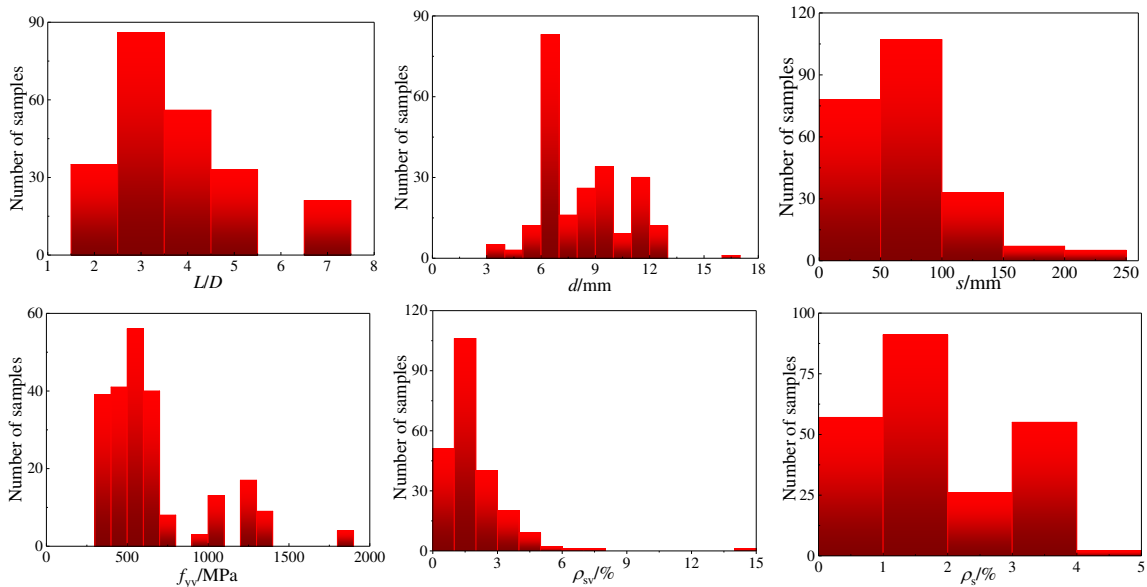
101 The compressive strength of concrete confined with spiral stirrups was related to the aspect
 102 ratio of specimens, the diameter, spacing, volumetric ratio and yield strength of spiral stirrups, the
 103 ratio of longitudinal reinforcement and the compressive strength of concrete. The range of
 104 influential parameters was listed in Table.1 and the distribution of the influential parameters were
 105 shown in Fig.1.

106 Table.1 Range of parameters in database

Variables	Minimum	Maximum	Mean	Correlation
L/D	1.67	6.97	3.80	-0.05
d/mm	3	16	7.97	-0.25
s/mm	10	240	66	-0.39
f_{yv}/MPa	307	1803	656	0.19
$\rho_{sv}/\%$	0.28	14.28	1.89	0.55
$\rho_s/\%$	0	4.8	1.66	-0.37
f_c/MPa	21	151	63.29	0.85
f_{cc}/MPa	19.3	259	78.44	1

107 Where, L/D was the aspect ratio of specimens, L was the height of specimens and D was the diameter of
 108 specimens; d was the diameter of stirrups; s was the spacing of stirrups; f_y was the yield strength of
 109 specimens; ρ_{sv} was the volumetric ratio of specimens; ρ_s was the ratio of longitudinal reinforcement; f_c
 110 was the compressive strength of concrete; f_{cc} was the compressive strength of confined concrete.

111



112

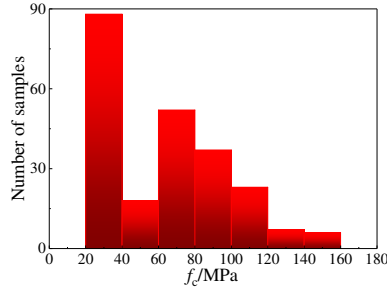


Fig.1 Distribution of influential parameters

113

114

115 3. Adaptive neuro-fuzzy inference system (ANFIS)

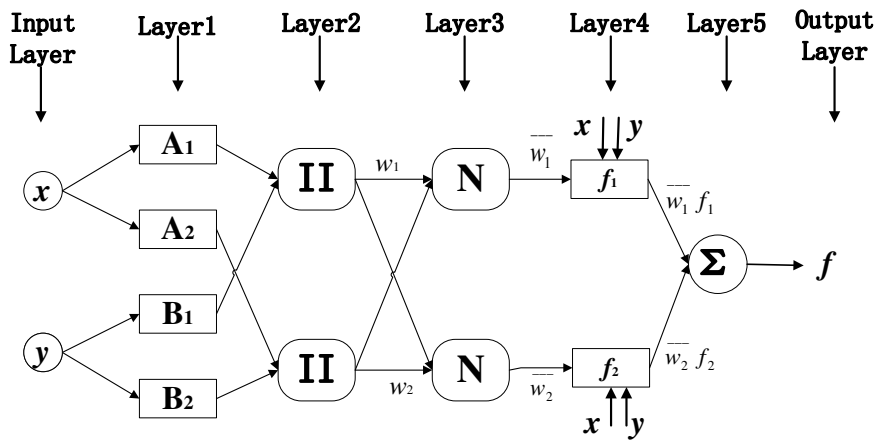
116 3.1 Conception

117 Adaptive neuro-fuzzy inference system (ANFIS) integrated the advantages of both neural
 118 networks and fuzzy logic systems with high self-adaptability and self learning ability to be
 119 identified as a universal estimator for responding to complex problems [16]. The ANFIS was a class
 120 of adaptive, multi-layer and feed-forward networks which was comprised of input-output varioubs
 121 and a fuzzy rule base of the Takagi-Sugeno type [21]. The ANFIS model incorporated the
 122 human-like reasoning style of fuzzy inference system through the use of input-output sets and a
 123 linguistic model consisting of a set of IF_THEN fuzzy rules, which was expressed as following:

124 Rule 1: IF x was A_1 and y was B_1 , THEN $f_1 = p_1x + q_1y + r_1$;

125 Rule 2: IF x was A_2 and y was B_2 , THEN $f_2 = p_2x + q_2y + r_2$;

126 The principle structures of ANFIS model was consisted of fiver layers, including input layer,
 127 input membership function layer, rule layer, output membership function layer and output layer
 128 [25]. The framework of different layers was different with each other, while the nodes of the same
 129 layer performed similarly to each other. The principle structures of ANFIS was shown in Fig.2.



130

131

Fig.2 The principle structures of ANFIS

132 Input layer: the influential parameters determined the number of nodes of the input layer. If
 133 the number of input variables was N , the number of input layer nodes was N .

134 Layer1: the membership function in this layer can fuzzy the input variables. Every node i in this
 135 layer was a square node with a membership function. The membership function was expressed in
 136 Eq.(1).

137

$$O_i^1 = \mu_{A_i}(x) \quad (1)$$

138 In which, x was the input variables, A_i was the fuzzy sets; O_i^1 was the subordinative function

139 values of A_i , which represented the degree belonging to A_i ; $\mu_{A_i}(x)$ was the membership function.

140 Layer2: the regular strength release layer. The nodes in this layer were responsibility for
 141 multiplying the input signals from the previous layer, meanwhile, the outputs of each node
 142 represented the credibility of the rules. The outputs of Layer2 were described in Eq.(2).

$$143 \quad \omega_i = \mu_{A_i}(x) \times \mu_{B_i}(y) \quad i = 1, 2 \quad (2)$$

144 Where, ω_i was the outputs of the Layer2.

145 Layer3: the normalization layer of rules. The i^{th} node calculates the ratio of the i^{th} rule firing strength
 146 to the sum of all rule firing strength. The outputs of Layer3 were shown in Eq.(3).

$$147 \quad \bar{\omega}_i = \frac{\omega_i}{(\omega_1 + \omega_2)} \quad i = 1, 2 \quad (3)$$

148 Where, $\bar{\omega}_i$ was the outputs of the Layer3 which also called normalized firing strength.

149 Layer4: calculating the outputs of fuzzy rules. Each node was an adaptive node and the output
 150 was given in Eq.(4).

$$151 \quad O_i^4 = \bar{\omega}_i f_i = \bar{\omega}_i (p_i x + q_i y + r_i) \quad i = 1, 2 \quad (4)$$

152 Where, O_i^4 was the output of Layer4; $\bar{\omega}_i$ was the output of Layer3; $\{p_i, q_i, r_i\}$ were parameter sets of
 153 nodes in Layer4.

154 Layer5: only had one fixed node to calculate the sum of total input signals. The total output of
 155 Layer5 was shown in Eq (5).

$$156 \quad O_i^5 = \sum \bar{\omega}_i f_i = \sum \bar{\omega}_i f_i / \sum \omega_i \quad i = 1, 2 \quad (5)$$

157 The O_i^5 also can be described as a linear combination of parameter sets of nodes in Layer4.

$$158 \quad \begin{aligned} O_i^5 &= \bar{\omega}_1 f_1 + \bar{\omega}_2 f_2 \\ &= (\bar{\omega}_1 x) p_1 + (\bar{\omega}_1 y) q_1 + (\bar{\omega}_1) r_1 + (\bar{\omega}_2 x) p_2 + (\bar{\omega}_2 y) q_2 + (\bar{\omega}_2) r_2 \end{aligned} \quad (6)$$

159 Output layer: the target values were obtained in this layer.

160 3.2 ANFIS model establishment

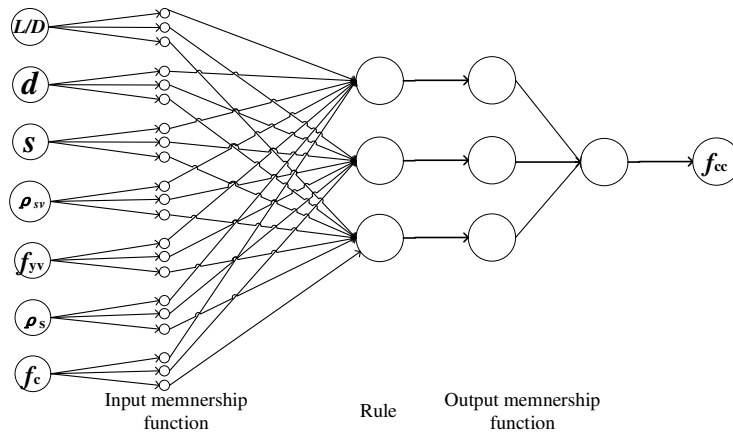
161 In this section, the ANFIS model for evaluating the compressive strength of concrete confined
 162 with spiral stirrups was established. The proposed ANFIS model was consisted of seven input
 163 parameters including the aspect ratio of specimens, the diameter, spacing, yield strength and
 164 volumetric ratio of stirrups, the ratio of longitudinal reinforcement and the compressive strength of
 165 concrete and one output variable (the compressive strength of confined concrete). The four
 166 membership functions including the triangular, trapezoidal, Gaussian and Π -shape were selected to
 167 construct the proposed ANFIS model, named as ANFISI, ANFISII, ANFISIII, ANFISIV, to obtain the
 168 suitable membership function, while the membership function in output layer was constant. The
 169 ANFIS mode was trained by 185-group data sets and tested by 46-group data sets, which were
 170 selected randomly. Up to 100 epochs were specified for the training process to obtain the minimum
 171 error tolerance. Furthermore, hybrid learning procedure which combined back-propagation
 172 gradient descent and least squares method for identification of premise and consequent parameters
 173 was adopted to establish the ANFIS model.

174 The performance of ANFIS model was examined by RMSE and R2 which were listed in Table.2.
 175 In Table.2, all ANFIS models had acceptable prediction performance. Among those models,
 176 ANFISIII constructed with Gaussian member function exhibited the best prediction performance,
 177 which the *RMSE* were 0.9986 and 0.9026 and the R^2 were 0.9986 and 0.9026 for training and testing
 178 phases. Thus, the ANFIS model constructed with Gaussian membership function was determined
 179 and the structures of the proposed ANFIS model was shown in Fig.3.

180

Table.2 The training and testing process of ANFIS model

Name	Training process		Testing process	
	<i>RMSE</i>	R^2	<i>RMSE</i>	R^2
ANFISI	2.28	0.9964	31.26	0.7122
ANFISII	4.84	0.9840	43.58	0.6274
ANFISIII	1.50	0.9986	3.87	0.9026
ANFISIV	6.04	0.9562	54.38	0.5764



181

182

Fig.3 Structures of proposed ANFIS model

183

3.3 Prediction performance validation

184

185

186

187

188

Fig.4 presented the comparison between the predicted results of the proposed ANFIS model and experimental results. In Fig.4, the prediction results from the proposed ANFIS model were well matched the experimental results in training and testing, which meant that the proposed models had good reliable and high performance for evaluating the compressive strength of concrete confined with stirrups.

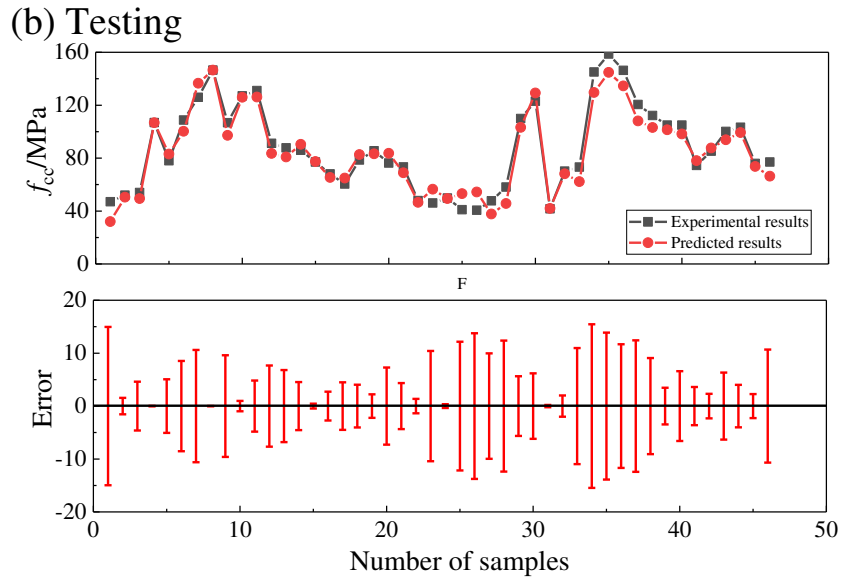
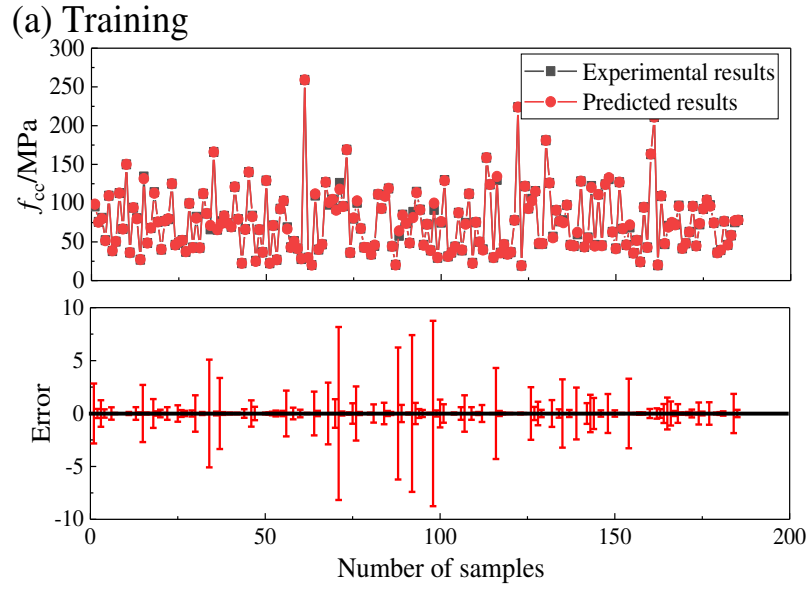


Fig.4 Comparison between predicted results and experimental results

192 4. Results and discussion

193 4.1 Results assessment criteria

194 A successfully trained ANFIS model should give an accurate output prediction, not only for
195 training process but also for new testing data. In this study, four assessment indicators were applied
196 to evaluate the prediction performance of the proposed ANFIS model, which were the root mean
197 square error ($RMSE$), coefficient of determination (R^2), integral absolute error (IAE) and
198 $\alpha 20$ -index [44], which were expressed in Eqs.(6)-(9).

$$199 \quad RMSE = \sqrt{\frac{1}{n} \sum_{k=1}^n (t_k - o_k)^2} \quad (6)$$

$$200 \quad R^2 = 1 - \left[\frac{\sum_{i=1}^n (t_i - o_i)^2}{\sum_{i=1}^n o_i^2} \right] \quad (7)$$

$$201 \quad IAE = \left(\sum_{k=1}^n (o_k - t_k)^2 \right)^{1/2} / \left(\sum_{k=1}^n o_k \right) \times 100\% \quad (8)$$

202
$$\alpha 20\text{-index} = 1 - \frac{n20}{n} \quad (9)$$

203 Where n was the total number of samples; t_k was the experimental result of k^{th} data; o_k was the
 204 output value of k^{th} data; $n20$ was the number of samples which the values of the
 205 $f_{cc,\text{predicted}} / f_{cc,\text{experiment}}$ were in the range of 0.8-1.2.

206 The value of R^2 was applied to evaluate the variation between predicted results and
 207 experimental results. The value of $RMSE$ and IAE were applied to evaluate the errors between
 208 predicted results and experimental results. The value of $\alpha 20\text{-index}$ was applied to evaluate the
 209 number of the predicted results falling in a deviation of compared with experimental results.
 210 Theoretically, the higher R^2 and lowest $RMSE$ and IAE indicated the good prediction performance of
 211 proposed models, while $\alpha 20\text{-index}$ was expected to 1 in the perfect prediction models.

212 *4.2 Existing prediction models for compressive strength of confined concrete*

213 In this section, four existing models proposed by Richart [5], Mander [7], Saatcioglu [10] and
 214 Legeron [3] for predicting the compressive strength of confined concrete were reviewed, listed in
 215 Table.3. In Table.3, the existing models for evaluating the compressive strength of concrete confined
 216 with stirrups were proposed by considering the effects of the compressive strength of concrete, the
 217 volumetric ratio and the yield strength of stirrups, which ignored the effects of the aspect ratio of
 218 specimens, the spacing and diameter of spiral stirrups, and the ratio of longitudinal reinforcements.
 219 On the other hand, those existing models were proposed based on a set of specific experimental
 220 results, when the new test data sets were introduced, the models may not performed well.

221 Table.3 Existing prediction models for compressive strength of confined concrete

Reference	Equations
Richart [5]	$f_{cc} = f_c + 2.05\rho_{sv}f_{yv}$
Mander [7]	$f_{cc} = f_c(-1.254 + 2.254\sqrt{1 + 7.94k_e f_{yv}\rho_{sv} / 2f_c} - k_e f_{yv}\rho_{sv} / f_c)$ $k_e = (1 - s / (2D)) / (1 - \rho_s)$
Saatcioglu [10]	$f_{cc} = f_c + k_1\rho_{sv}f_{yv} / 2$ $k_1 = 6.7(\rho_{sv}f_{yv} / 2)^{-0.17}$
Legeron [3]	$f_{cc} = f_c [1 + 2.4(I_e)^{0.7}]$ $I_e = 0.5k_e\rho_{sv}f_{yv} / f_c$

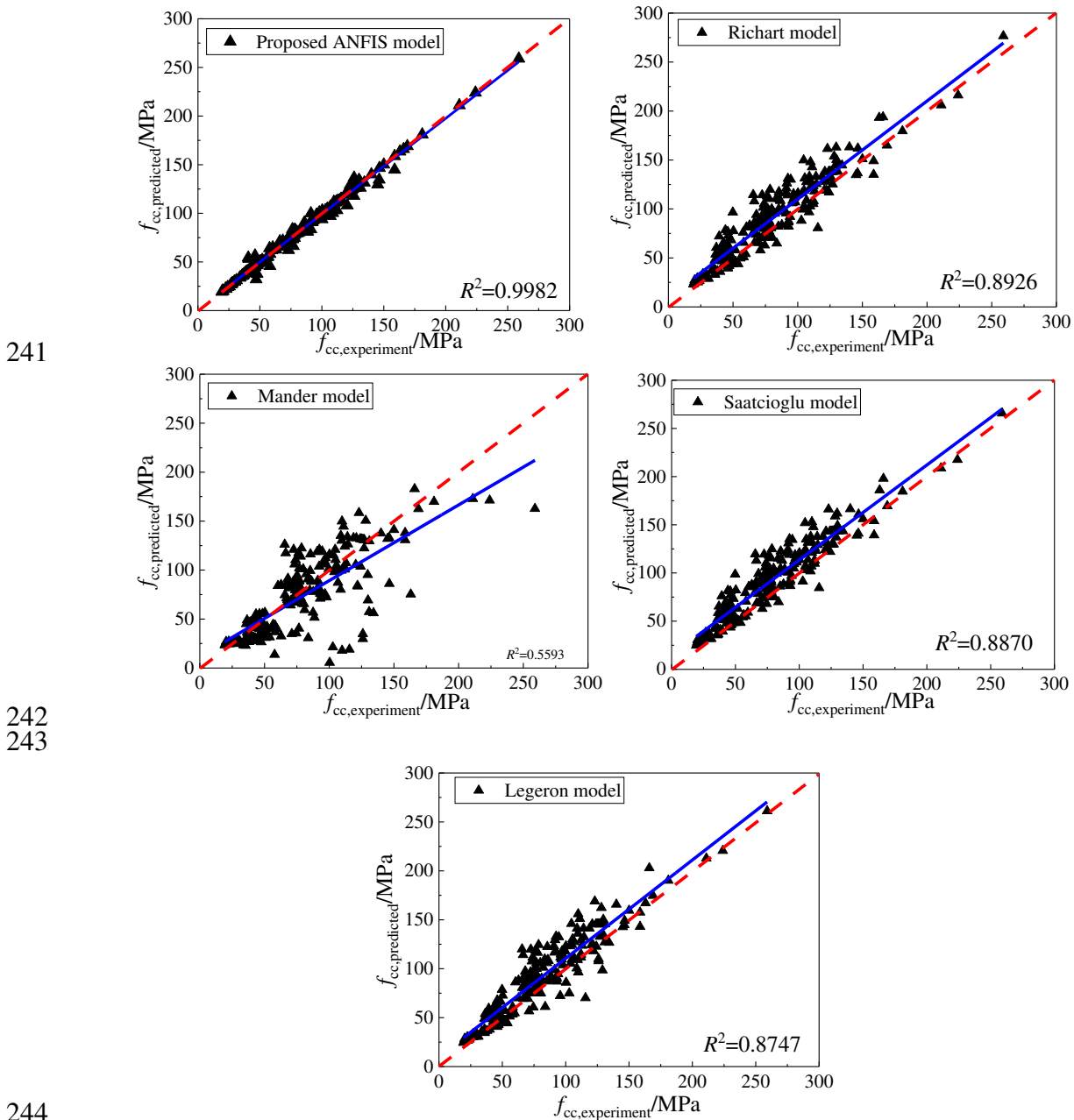
222 Where, f_{cc} was the compressive strength of confined concrete; f_c was the compressive strength of concrete;
 223 ρ_{sv} was the volumetric ratio of stirrups; f_{yv} was the yield strength of stirrups; k_e was the effective
 224 confinement coefficient; s was the spacing of stirrups; D was the diameter of specimens; ρ_s was the ratio of
 225 longitudinal reinforcement; k_1 was the parameter related to the yield strength and the volumetric ratio of
 226 stirrups.

227 *4.3 Results and discussion*

228 Fig.5 showed the comparison of compressive strength of concrete confined with stirrups of
 229 existing and proposed prediction models (listed in Table.3) and experimental results. The 45 degree
 230 line indicated that the perfect predicted results, equaling the experimental results. It was obvious

231 that the compressive strength of concrete confined with stirrups calculated from the all existing
 232 models was lower than the experiment results, which can be attributed to the effects of concrete
 233 strength on the shear strength of concrete were underestimated and the ultimate shear strength of
 234 concrete fluctuated heavily, the upper limited value of the compressive strength of concrete confined
 235 with stirrups was derived as the lower limited value of experimental results in existing models.

236 The predicted results from the proposed models were also compared with experimental results.
 237 In Fig.5, the scatter of proposed models in this study approximated to the experimental results.
 238 Moreover, Fig.6 showed that the histograms of the proposed models, demonstrating that the good
 239 distribution with the mean values of unity.
 240



245 Fig.5 Comparison ultimate shear strength of concrete of prediction models and experimental results

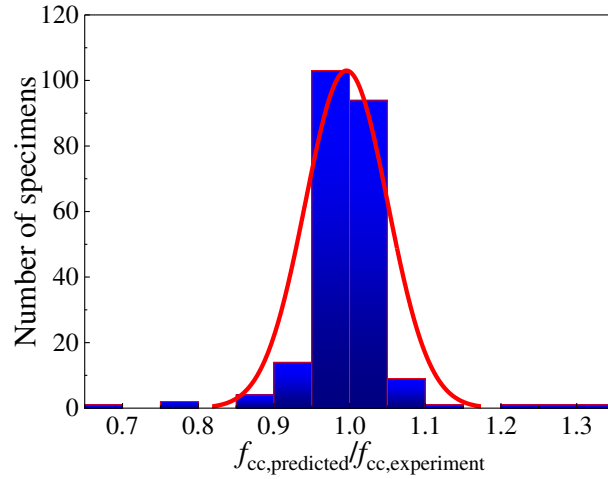
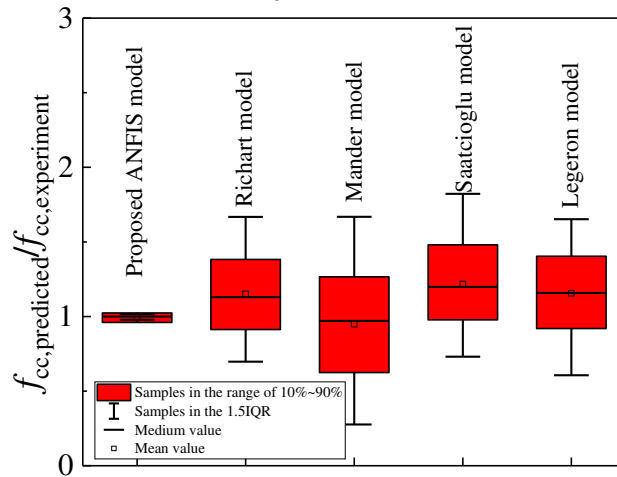


Fig.6 Histograms of the proposed models

246
247

248 Fig.7 showed that the box plot of $f_{cc,predicted}/f_{cc,experiment}$ with different prediction models and
249 Table.4 listed the performance indicators of different models. It was highlighted that the proposed
250 models were suitable for evaluating the compressive strength of concrete confined with stirrups due
251 to the lowest *RMSE*, *IAE* and *SD* and the unity of mean values.



252
253

Fig.7 Box plot of $f_{cc,predicted}/f_{cc,experiment}$ with different prediction models

254

Table.4 Performance indicators of different prediction models

Models	R^2	<i>RMSE</i>	<i>IAE</i>	$f_{cc,predicted}/f_{cc,experiment}$		
				Mean	<i>SD</i>	$\alpha 20$ -index
Proposed ANFIS model	0.9982	3.72	0.02	0.9959	0.05	0.99
Richart	0.9699	16.93	0.15	1.1510	0.20	0.63
Mander	0.8794	28.79	0.25	0.9486	0.30	0.63
Saatcioglu	0.9626	19.50	0.17	1.2172	0.21	0.50
Legeron	0.9659	18.14	0.16	1.1556	0.19	0.59

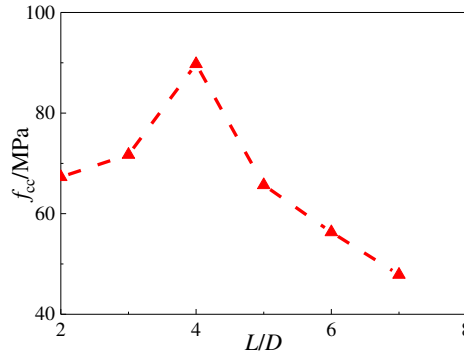
255 5. Parameter Analysis

256 In this study, the effects of the investigated parameters including the aspect ratio of specimens,
257 the diameter, spacing, yield strength and volumetric ratio of stirrups, the ratio of longitudinal
258 reinforcement and the compressive strength of concrete were performed based on the proposed
259 ANFIS models. The mean values (listed in Table.1) of the investigated parameters were set as the

260 basic values, while the certain parameter was varied from the minimum value to the maximum
261 value. The outputs were obtained from the proposed ANFIS model.

262 5.1 Aspect ratio of specimens

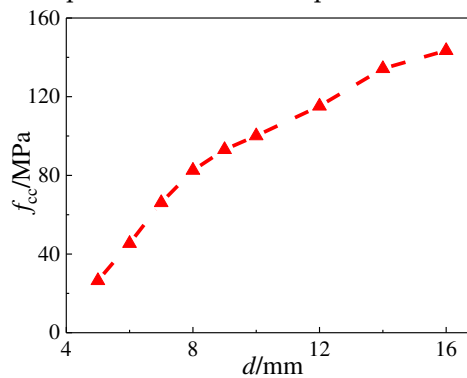
263 Fig.8 showed the relationships between the compressive strength of confined concrete and the
264 aspect ratio of specimens. The compressive strength of confined concrete increased firstly and then
265 decreased with the increase of the aspect ratio of specimens.



266
267 Fig.8 The compressive strength of confined concrete varied with the aspect ratio of specimens

268 5.2 Diameter of stirrups

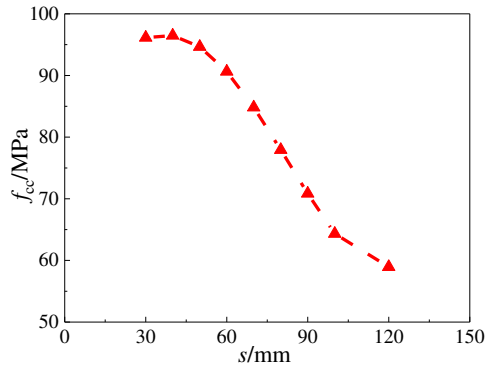
269 Fig.9 showed that the compressive strength of confined concrete varied with the diameter of
270 stirrups. The increase of the diameter of stirrups enhanced the confinement area of specimens. Thus,
271 the increase of the diameter of stirrups enhanced the compressive strength of confined concrete.



272
273 Fig.9 The compressive strength of confined concrete varied with the diameter of stirrups

274 5.3 Spacing of stirrups

275 Fig.10 presented that the compressive strength of confined concrete varied with the spacing of
276 stirrups. The increase of the spacing of stirrups declined the effective confinement area of specimens
277 and the longitudinal reinforcement tended to be bucking failure, which decreased the compressive
278 strength of confined concrete.



279

280

Fig.10 The compressive strength of confined concrete varied with the spacing of stirrups

281

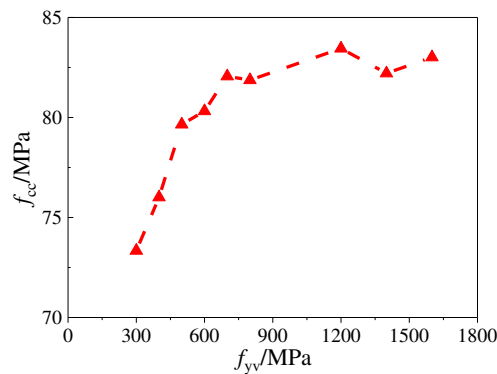
5.4 Yield strength of stirrups

282

In Fig.11, the increase of the yield strength of stirrups enhanced the compressive strength of confined concrete. However, when the yield strength of stirrups exceeded 700MPa, the compressive strength of confined concrete increased slowly.

283

284



285

286

Fig.11 The compressive strength of confined concrete varied with the yield strength of stirrups

287

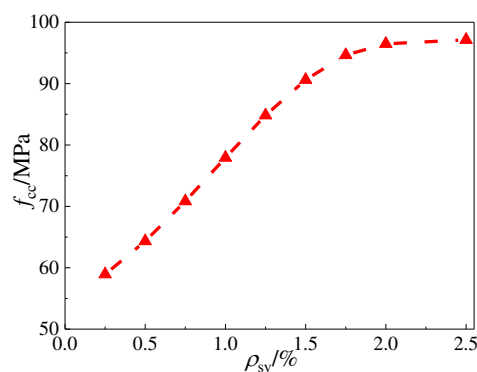
5.5 Volumetric ratio of stirrups

288

In Fig.12, the increment of the volumetric ratio of stirrups improved the compressive strength of confined concrete. The increment of the volumetric ratio of stirrups enhanced the lateral confinement of stirrups, which improved the compressive strength of confined concrete.

289

290



291

292

Fig.12 The compressive strength of confined concrete varied with the volumetric ratio of stirrups

293

5.6 Ratio of longitudinal reinforcement

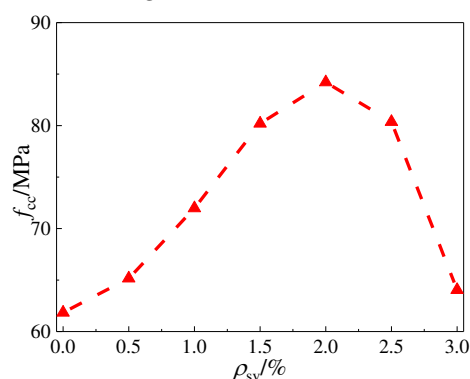
294

Fig.13 showed that the compressive strength of confined concrete varied with the ratio of longitudinal reinforcement. When the ratio of longitudinal reinforcement was lower than 2%, the ratio of longitudinal reinforcement improved the compressive strength of confined concrete. When

295

296

297 the ratio of longitudinal reinforcement was over 2%, the ratio of longitudinal reinforcement had the
298 negative effects on the compressive strength of confined concrete.

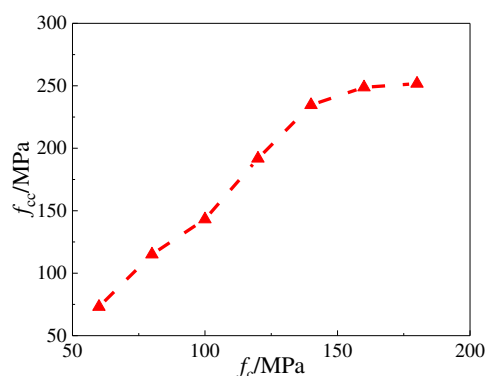


299

300 Fig.13 The compressive strength of confined concrete varied with the ratio of longitudinal reinforcement

301 5.7 Compressive strength of concrete

302 Fig.14 showed that the compressive strength of confined concrete varied with the compressive
303 strength of concrete. The compressive strength of confined concrete increased with the increase of
304 concrete, while the increment of the compressive strength of confinement increased slowly when the
305 compressive strength of concrete was more than 140 MPa.



306

307 Fig.14 The compressive strength of confined concrete varied with the compressive strength of concrete

308 6. Conclusions

309 The aim of this paper was to evaluate the compressive strength of concrete confined with
310 spiral stirrups. A reliable database consisting of 231-group experimental results collected from
311 previous studies was established and the ANFIS model for evaluating the compressive strength of
312 confined concrete was developed. The parametric analysis was performed based on the ANFIS
313 model. The conclusions were drawn as following:

314 (1) The ANFIS model was adopted to predict the compressive strength of concrete confined
315 with spiral stirrups, which has high prediction performance for both training and testing data sets.

316 (2) The ANFIS model proposed in this study has high reliability and high applicable in
317 predicting the compressive strength of confined concrete by comparing with the existing models.

318 (3) Based on the proposed ANFIS model, the effects of influential parameters including the
319 aspect ratio of specimens, the diameter, spacing, yield strength and volumetric ratio of stirrups, the
320 ratio of longitudinal reinforcement, and the compressive strength of concrete on the compressive
321 strength of confined concrete were analyzed.

322 Compliance with Ethical Standard :

323 Funding: This research was funded by National Science Foundation of China, grant number 51678190.

324 Conflicts of Interest: The authors declare no conflict of interest.

325 **References**

- 326 1. Nemecek, J.; Padevet, P.; Patzák, B. Effect of transversal reinforcement in normal and high strength
327 concrete columns. *Materials and Structures*, **2005**, 38(7), 665-671.
- 328 2. Saatcioglu, M.; Razvi, S.R. High-Strength Concrete Columns With Square Sections Under Concentric
329 Compression. *Journal of Structural Engineering*, **1998**, 124(12), 1438-1447.
- 330 3. Légeron, F.; Paultre, P. Uniaxial Confinement Model for Normal- and High-Strength Concrete Columns.
331 *Journal of Structural Engineering*, **2003**, 129(2), 241-252.
- 332 4. Richart, F.E.; Brandtzæg, A.; Brown, R.L. Failure of plain and spirally reinforced concrete in compression.
333 *Bull.university of Illinois Engrg.experiment Station*, **1929**, 26.
- 334 5. Richart, F.E.; Brandtzæg, A.; Brown, R.L. A study of the failure of concrete under combined compressive
335 stresses. *Uni.illinois Eng.exp.st.bull*, **1928**, 185.
- 336 6. Mander, J.B.; Priestley, M.J.N.; Park, R. Observed Stress-Strain Behavior of Confined Concrete. *Journal of*
337 *Structural Engineering*, **1988**, 114(8),1827-1849.
- 338 7. Mander, J.B.; Priestley, M.J.N.; Park, R. Theoretical Stress-Strain Model for Confined Concrete. *Journal of*
339 *Structural Engineering*, **1988**, 114(8), 1804-1826.
- 340 8. Cusson D.; Paultre P. High-strength concrete columns confined by rectangular ties. *Journal of Structural*
341 *Engineering*, 1994, 120(3): 783-804.
- 342 9. Bing L.; Park H. Stress-strain behavior of high-strength concrete confined by normal-strength transverse
343 reinforcements. *ACI Structural Journal*, 2001, 98(3): 395-406.
- 344 10. Saatcioglu, M.; Razvi, S.R. Strength and Ductility of Confined Concrete. *Journal of Structural Engineering*,
345 **1992**, 118(6), 1590-1607.
- 346 11. Sharma U.K.; Bhagava P.; Kaushik S.K. Behavior of confined high strength concrete columns under axial
347 compression. *Journal of Advanced Concrete Technology*, 2005, 3(2): 267-281.
- 348 12. Wang G. Factors of binding effect on high-strength stirrup confined concrete under axial compression.
349 *Earthquake Resistant Engineering and Retrofitting*, 2014, 36(2): 119-123,
- 350 13. Wei Y.; Wu Y.F. Compression behavior of concrete columns confined by high strength steel wire.
351 *Construction and Building Materials*, 2014, 54(15): 443-453.
- 352 14. Li Y.Z.; Cao S.Y.; Liang H. Axial compressive behavior of concrete columns with grade 600 MPa
353 reinforcing bars. *Engineering Structures*, 2018, 172(1): 497-507
- 354 15. Deng Z.C.; Yao J.S. Axial compression behavior of ultra-high performance concrete columns confined by
355 high-strength stirrups. *Acta Materiae Compositae Sinica*, 2020, 10: 2590-2601.
- 356 16. Yalpir, S.; Ozkan, G. Knowledge-based FIS and ANFIS models development and comparison for
357 residential real estate valuation. *International Journal of Strategic Property Management*, **2018**, 22(2), 110-118.
- 358 17. Akbarpour H.; Akbarpour M. Prediction of punching shear strength of two-way slabs using artificial
359 neural network and adaptive neuro-fuzzy inference system. *Neural Computing and Application*, 2017, 28:
360 3273-3284.
- 361 18. Khademi F.; Jamal S.M.; Deshpande N.; Londhe S. Prediction of strength of recycled aggregate concrete
362 using artificial neural network, adaptive neuro-fuzzy inference system and multiple linear regression.
363 *International Journal of Sustainable Built Environment*, 2016, 5: 355-369.
- 364 19. Bilgehan M. A comparative study for the concrete compressive strength estimation using neural network
365 and neuro-fuzzy modelling approaches. *Nondestructive Testing and Evaluation*, 2011, 26(01): 35-55.
- 366 20. Vakhshouri B.; Nejadi S. Prediction of compressive strength of self-compacting concrete by ANFIS
367 models. *Neurocomputing*, 2018, 280(6):13-22.
- 368 21. Jiang J.S.R. ANFIS: adaptive-network-based fuzzy inference system. *IEEE Transactions on Systems, Man*
369 *and Cybernetics*, 1993, 23(3): 665-685.
- 370 22. Sakai, J. Effect of lateral confinement of concrete and varying the axial load on seismic response of bridges,
371 *Doctor of Engineering Dissertation, Department of Civil Engineering, Tokyo Institute of Technology, Tokyo. 2001*
- 372 23. Sakai, J.; Kawashima, K.; Une, H.; Yoneda, K. Effect of tie spacing on the stress-strain relation of confined
373 concrete, *Journal of Structural Engineering. ASCE. 2000*,46 (3), 757-766.
- 374 24. Antonius. Performance of high-strength concrete columns confined by the medium strength of spirals and
375 hoops, *Asian Journal Civil Engineering. 2014*,15 (2), 245-258.
- 376 25. Assa, B.; Nishiyama, M.; Watanabe, F. New Approach for modeling confined concrete I: circular columns,
377 *Journal of Structural Engineering. ASCE. 2001*,127 (7), 743-750.

- 378 26. Bing, L. Strength and ductility of reinforced concrete members and frames constructed using high strength
379 concrete, *Civil Engineering at the University of Canterbury, Christchurch, New Zealand*. **1993**.
380 27. Yang, X.; Zohrevand, P.; Mirmiran, A.; Behavior of ultrahigh-performance concrete confined by steel,
381 *Journal of Materials in Civil Engineering*. **2016**, 28 (10), 04016113
382 28. Cusson, D.; Larrard, F.D.; Boulay, C.; Paultre, P. Strain localization in confined high-strength concrete
383 columns, *Journal of Structural Engineering. ASCE*. **1998**,124 (9), 1055-1061.
384 29. Montgomery, D.L. Behavior of spirally reinforced high strength concrete columns under axial loading,
385 *Doctoral and Master thesis, National Library of Canada*. **1996**.
386 30. Toklucu, M.T. Behavior of Reinforced Concrete Columns Confined with Circular Spirals and Hoops,
387 *University of Toronto*. **1992**
388 31. Sheikh, S.A.; Toklucu, M.T. Reinforced Concrete Columns Confined by Circular Spirals and Hoops, *ACI*
389 *Struct. J.* **1993**,90 (5): 542-553.
390 32. Silva, P.D. Effect of concrete strength on axial load response of circular columns, *McGill University, Canada*.
391 **2000**.
392 33. Wang, Y.; Zhang, Z.; Zheng, W.Z, Zhu, A.P.; Zhao, J. Mechanical behavior of concrete columns confined
393 by steel bar for prestressed concrete spiral hoops, *J. Harbin Institute. Tech.* **2013**,45 (4): 6-13
394 34. Razvi, S.R. Confinement of normal and high-strength concrete columns. *Univ. Ott, Can.* **1995**.
395 35. Wei, Y.; Wu, Y.F. Compression behavior of concrete columns confined by high strength steel wire.
396 *Construction & Building Materials*, **2014**, 54(11):443-453.
397 36. Wang, W.; Zhang, M.; Tang, T. Behaviour of high-strength concrete columns confined by spiral
398 reinforcement under uniaxial compression. *Construction & Building Materials*, **2017**, 154:496–503.
399 37. Marvel, L.; Doty, N.; Lindquist, W. Axial behavior of high-strength concrete confined with multiple spirals.
400 *Engineering Structures*, **2014**, 60(2):68-80

401 Appendix

402 A database consisting of 231 experimental results of concrete confined with spiral stirrups
403 collected from the previous studies was established.

404 Table.5 Experimental Data used for establishing Compressive Strength ANFIS Model

No.	L/D	Transverse reinforcements				ρ_s /%	f_c	f_{cc}	Reference
		d/mm	s/mm	f_{yv} /MPa	ρ_{sv} /%				
1	3.42	12	52	310	1.99	1.60	24.00	38.00	[6]
2	3.42	12	52	340	1.99	1.60	30.00	48.00	[6]
3	3.42	12	52	340	1.99	1.60	32.00	47.00	[6]
4	3.42	12	41	340	2.52	1.60	29.00	51.00	[6]
5	3.42	12	69	340	1.50	1.60	29.00	46.00	[6]
6	3.42	12	103	340	1.00	1.60	29.00	40.00	[6]
7	3.42	10	119	320	0.60	1.59	29.00	36.00	[6]
8	3.42	10	36	320	1.98	1.59	29.00	47.00	[6]
9	3.42	16	93	307	1.97	1.63	29.00	46.00	[6]
10	3.42	12	52	340	1.99	3.27	32.00	52.00	[6]
11	3.42	12	52	340	1.99	3.30	30.00	49.00	[6]
12	3.42	12	52	340	1.99	2.34	32.00	52.00	[6]
13	3.42	12	52	340	1.99	3.20	30.00	50.00	[6]
14	3.42	12	52	340	1.99	4.80	30.00	54.00	[6]
15	3.42	12	52	340	1.99	3.20	32.00	52.00	[6]
16	3.24	6.4	120	376	0.57	1.18	24.60	29.60	[22]
17	3.24	6.4	60	376	1.16	1.18	24.60	29.40	[22]
18	3.24	6.4	40	376	1.71	1.18	24.60	35.90	[22]
19	3.24	9.0	240	376	0.57	1.18	24.60	31.10	[22]
20	3.24	9.0	120	376	1.14	1.18	24.60	36.00	[22]
21	3.24	9.0	80	376	1.71	1.18	24.60	36.10	[22]

22	3.21	6.4	20	363	2.26	1.85	21.00	35.40	[23]
23	3.21	6.4	30	363	1.51	1.85	21.00	29.70	[23]
24	3.21	6.4	40	363	1.14	1.85	21.00	27.00	[23]
25	3.21	6.4	60	363	0.75	1.85	21.00	24.00	[23]
26	3.21	6.4	80	363	0.57	1.85	21.00	22.80	[23]
27	3.21	6.4	120	363	0.38	1.85	21.00	19.80	[23]
28	3.21	6.4	160	363	0.28	1.85	21.00	19.30	[23]
29	3.21	9.0	40	363	2.26	1.85	21.00	33.80	[23]
30	3.21	9.0	60	363	1.51	1.85	21.00	27.80	[23]
31	3.21	9.0	80	363	1.13	1.85	21.00	25.40	[23]
32	3.21	9.0	120	363	0.75	1.85	21.00	22.30	[23]
33	3.21	9.0	160	363	0.57	1.85	21.00	20.10	[23]
34	3.21	11.0	60	363	2.26	1.85	21.00	34.10	[23]
35	3.21	11.0	80	363	1.70	1.85	21.00	26.70	[23]
36	3.21	11.0	120	363	1.13	1.85	21.00	22.40	[23]
37	3.21	11.0	160	363	0.85	1.85	21.00	20.30	[23]
38	5.00	6.25	35	488	4.38	3.60	51.80	80.99	[24]
39	5.00	6.25	35	488	4.38	3.60	63.20	97.95	[24]
40	5.00	5.5	35	315	3.19	3.60	63.20	74.36	[24]
41	5.00	5.5	55	315	2.03	3.60	63.20	65.77	[24]
42	5.00	6.25	35	488	4.38	3.60	75.30	122.07	[24]
43	5.00	6.25	35	587	4.38	3.60	75.30	121.79	[24]
44	5.00	6.25	55	587	2.79	3.60	75.30	106.84	[24]
45	2.07	6.25	28	1296	3.05	0	25.04	95.70	[25]
46	2.07	6.25	44	1296	1.92	0	25.04	57.83	[25]
47	2.07	6.25	20	1296	4.15	0	34.13	129.03	[25]
48	2.07	6.25	28	1296	3.04	0	34.13	100.34	[25]
49	2.07	6.25	47	1296	1.80	0	34.13	62.87	[25]
50	2.07	6.25	50	909	1.69	0	34.13	58.19	[25]
51	2.07	6.25	75	909	1.13	0	34.13	42.28	[25]
52	2.07	6.25	28	1296	3.05	0	41.38	109.94	[25]
53	2.07	6.25	44	1296	1.92	0	41.38	76.59	[25]
54	2.07	6.25	28	1296	3.05	0	49.75	125.98	[25]
55	2.07	6.25	44	1296	1.92	0	49.75	88.61	[25]
56	2.07	6.25	28	1296	3.02	0	64.40	134.25	[25]
57	2.07	6.25	28	1296	3.05	0	64.40	130.87	[25]
58	2.07	6.25	44	1296	1.92	0	64.40	96.74	[25]
59	2.07	6.25	28	1296	3.02	0	70.10	130.00	[25]
60	2.07	6.25	44	1296	1.92	0	70.10	91.18	[25]
61	2.07	6.25	21	1296	4.15	0	83.03	163.01	[25]
62	2.07	6.25	28	1296	3.01	0	83.03	129.74	[25]
63	2.07	6.25	47	1296	1.82	0	83.03	105.48	[25]
64	2.07	6.25	50	909	1.69	0	83.03	99.64	[25]
65	3.43	6	20	445	2.69	1.5	63.00	93.00	[26]
66	3.43	6	35	445	1.54	1.5	63.00	78.00	[26]
67	3.43	6	50	445	1.08	1.5	63.00	74.70	[26]
68	3.43	6	65	445	0.83	1.5	63.00	70.60	[26]
69	3.43	6	20	445	2.69	1.5	72.30	108.80	[26]
70	3.43	6	35	445	1.54	1.5	72.30	92.70	[26]
71	3.43	6	50	445	1.08	1.5	72.30	85.00	[26]
72	3.43	6	65	445	0.83	1.5	72.30	73.80	[26]
73	3.43	6.4	20	1318	2.94	1.5	52.00	126.00	[26]

74	3.43	6.4	35	1318	1.67	1.5	52.00	87.50	[26]
75	3.43	6.4	50	1318	1.17	1.5	52.00	68.50	[26]
76	3.43	6.4	20	1318	2.94	1.5	82.50	146.50	[26]
77	3.43	6.4	35	1318	1.67	1.5	82.50	106.80	[26]
78	3.43	6.4	50	1318	1.17	1.5	82.50	92.30	[26]
79	3.43	6.4	35	1318	1.68	1.5	35.20	115.60	[26]
80	3.43	6.4	53	1318	1.10	1.5	35.20	83.80	[26]
81	3.43	6.4	70	1318	0.84	1.5	35.20	71.10	[26]
82	2.04	5.1	51	414	1.65	0	151.00	169.00	[27]
83	2.04	5.1	25	414	3.37	0	151.00	181.00	[27]
84	2.04	5.1	13	414	6.48	0	151.00	211.00	[27]
85	2.04	7.6	38	414	5.05	0	151.00	166.00	[27]
86	2.04	7.6	25	414	7.68	0	151.00	224.00	[27]
87	2.04	7.6	13	414	14.80	0	151.00	259.00	[27]
88	3.45	6	36	580	2.20	0	112.00	127.00	[28]
89	3.45	6	36	580	2.20	0	112.00	126.00	[28]
90	3.45	6	36	580	2.20	0	66.00	94.00	[28]
91	3.45	6	36	580	2.20	0	92.00	113.00	[28]
92	3.45	5	51	588	1.10	0	92.00	112.00	[28]
93	2.22	6	36	580	2.20	0	112.00	131.00	[28]
94	6.94	6	36	580	2.20	0	112.00	121.00	[28]
95	3.26	6	29	580	2.20	0	112.00	124.00	[28]
96	3.47	6	18	580	4.30	0	112.00	140.00	[28]
97	3.45	5	51	588	1.10	0	112.00	127.00	[28]
98	3.47	6	36	580	2.20	2	112.00	125.00	[28]
99	3.45	6	36	580	2.20	4	112.00	127.00	[28]
100	4.00	11.3	41	522	1.17	3	69.70	93.00	[29]
101	4.00	11.3	53	522	3.62	3	69.70	86.50	[29]
102	4.00	11.3	79	522	2.43	3	69.70	91.20	[29]
103	4.00	11.3	109	522	1.76	3	69.70	75.20	[29]
104	4.00	8	41	666	2.23	3	69.70	76.40	[29]
105	4.00	8	53	666	1.73	3	69.70	75.80	[29]
106	4.00	8	79	666	1.16	3	69.70	78.20	[29]
107	4.00	8	109	666	0.84	3	69.70	76.40	[29]
108	4.00	5.7	41	583	1.17	3	69.70	87.70	[29]
109	4.00	5.7	53	583	0.91	3	69.70	79.40	[29]
110	4.00	11.3	64	522	3.77	3.1	69.70	85.90	[29]
111	4.00	9.5	43	508	3.96	3.1	69.70	83.50	[29]
112	4.00	9.5	64	508	2.66	3.1	69.70	77.00	[29]
113	4.00	9.5	86	508	1.98	3.1	69.70	74.10	[29]
114	4.00	8	64	666	1.79	3.1	69.70	68.10	[29]
115	4.00	6.4	43	646	1.76	3.1	69.70	72.30	[29]
116	4.00	6.4	64	646	1.18	3.1	69.70	66.90	[29]
117	4.00	6.4	86	646	0.88	3.1	69.70	60.40	[29]
118	4.00	4.8	43	692	0.96	3.1	69.70	62.80	[29]
119	4.00	11.3	43	522	5.61	3.1	89.80	104.60	[29]
120	4.00	11.3	64	522	3.77	3.1	89.80	94.60	[29]
121	4.00	11.3	86	522	2.81	3.1	89.80	78.60	[29]
122	4.00	9.5	43	508	3.96	3.1	89.80	92.40	[29]
123	4.00	9.5	64	508	2.66	3.1	89.80	85.50	[29]
124	4.00	9.5	86	508	1.98	3.1	89.80	77.90	[29]
125	4.00	8	43	666	2.67	3.1	89.80	91.60	[29]

126	4.00	8	64	666	1.79	3.1	89.80	72.50	[29]
127	4.00	8	86	666	1.33	3.1	89.80	66.40	[29]
128	4.00	6.4	43	646	1.76	3.1	89.80	76.30	[29]
129	4.00	6.4	64	646	1.18	3.1	89.80	74.00	[29]
130	4.00	6.4	86	646	0.88	3.1	89.80	73.30	[29]
131	4.00	4.8	43	692	1.74	3.1	89.80	65.60	[29]
132	4.00	11.3	56	452	2.38	2.3	35.90	51.90	[30,31]
133	4.00	11.3	76	452	1.75	2.3	35.90	48.50	[30,31]
134	4.00	11.3	112	452	1.19	2.3	35.90	41.50	[30,31]
135	4.00	11.3	152	452	0.88	2.3	35.90	43.00	[30,31]
136	4.00	10.1	56	607	1.89	2.3	35.90	44.60	[30,31]
137	4.00	10.1	76	607	1.39	2.3	35.90	47.90	[30,31]
138	4.00	10.1	112	607	0.95	2.3	35.90	46.70	[30,31]
139	4.00	5.7	56	593	0.60	2.3	35.90	46.10	[30,31]
140	4.00	11.3	79	452	2.55	1.5	35.50	42.80	[30,31]
141	4.00	11.3	109	452	1.85	1.5	35.50	38.90	[30,31]
142	4.00	11.3	41	607	4.91	1.5	35.50	49.80	[30,31]
143	4.00	10.1	53	607	3.02	1.5	35.50	46.50	[30,31]
144	4.00	10.1	79	607	2.03	1.5	35.50	43.80	[30,31]
145	4.00	10.1	109	607	1.47	1.5	35.50	36.50	[30,31]
146	4.00	5.7	41	593	1.23	1.5	35.50	41.30	[30,31]
147	4.00	5.7	53	593	0.95	1.5	35.50	41.00	[30,31]
148	4.00	10.1	64	607	3.36	3.1	34.90	46.00	[30,31]
149	4.00	6.4	64	629	1.32	3.1	34.90	40.30	[30,31]
150	4.00	6.4	64	629	1.32	3.1	34.90	38.90	[30,31]
151	4.00	6.4	86	629	0.98	3.1	34.90	35.90	[30,31]
152	4.00	6.4	43	629	1.96	3.1	34.90	46.00	[30,31]
153	4.00	6.4	43	629	1.96	3.1	34.90	44.80	[30,31]
154	4.00	6.4	43	629	1.96	3.1	34.90	46.00	[30,31]
155	4.00	4.8	43	605	1.01	3.1	34.90	40.60	[30,31]
156	5.25	11.3	100	440	1.40	2.6	35.50	47.00	[32]
157	5.25	9.5	100	560	1.00	2.6	35.50	47.70	[32]
158	5.25	11.3	100	440	1.40	2.6	39.50	56.60	[32]
159	5.25	9.5	100	560	1.00	2.6	39.50	58.10	[32]
160	5.25	11.3	75	440	1.86	2.6	59.60	67.10	[32]
161	5.25	9.5	80	560	1.24	2.6	59.60	67.80	[32]
162	5.25	11.3	45	440	3.11	2.6	119.90	109.90	[32]
163	5.25	9.5	50	560	1.99	2.6	119.90	111.10	[32]
164	5.25	11.3	35	440	4.00	2.6	125.40	123.00	[32]
165	5.25	9.5	40	560	2.48	2.6	125.40	128.20	[32]
166	5.00	9	70	1034	2.42	1.44	27.20	44.10	[33]
167	5.00	9	80	1034	2.12	1.44	27.20	39.30	[33]
168	5.00	9	100	1034	1.70	1.44	41.50	50.30	[33]
169	5.00	9	200	1034	0.85	1.44	41.50	43.40	[33]
170	5.00	9	70	768	2.42	1.44	27.20	42.80	[33]
171	5.00	9	80	768	2.12	1.44	27.20	37.10	[33]
172	5.00	9	100	768	1.70	1.44	41.50	48.50	[33]
173	5.00	9	200	768	0.85	1.44	41.50	42.70	[33]
174	5.00	7	50	726	2.05	1.44	27.20	45.30	[33]
175	5.00	7	60	726	1.71	1.44	27.20	40.00	[33]
176	5.00	7	100	726	1.03	1.44	41.50	44.70	[33]
177	5.00	7	200	726	0.51	1.44	41.50	41.70	[33]

178	5.00	7	50	1027	2.05	1.44	27.20	47.50	[33]
179	5.00	7	60	1027	1.71	1.44	27.20	41.50	[33]
180	5.00	7	100	1027	1.03	1.44	41.50	46.10	[33]
181	5.00	7	200	1027	0.51	1.44	41.50	42.20	[33]
182	6.70	6.3	135	660	0.41	0	60.00	70.20	[34]
183	6.70	11.3	135	400	1.35	0	60.00	73.20	[34]
184	6.70	6.3	70	660	0.80	0	60.00	80.40	[34]
185	6.70	6.3	70	660	0.80	0	60.00	79.20	[34]
186	6.70	6.3	70	660	0.80	3.27	60.00	72.60	[34]
187	6.70	6.3	135	660	0.41	3.27	60.00	66.60	[34]
188	6.70	6.3	70	660	0.80	0	124.00	145.10	[34]
189	6.70	11.3	135	400	1.35	0	124.00	158.70	[34]
190	6.70	11.3	60	400	3.05	0	124.00	158.70	[34]
191	6.70	6.3	60	660	0.93	0	124.00	146.30	[34]
192	6.70	7.5	60	1000	1.32	0	124.00	150.00	[34]
193	6.70	7.5	60	1000	1.32	0	92.00	120.50	[34]
194	6.70	11.3	60	400	3.05	0	92.00	124.20	[34]
195	6.70	7.5	100	1000	0.79	0	92.00	112.20	[34]
196	6.70	7.5	60	1000	1.32	3.27	92.00	104.90	[34]
197	6.70	7.5	100	1000	0.79	3.27	92.00	97.50	[34]
198	6.70	11.3	100	400	1.83	0	92.00	111.30	[34]
199	6.70	6.3	100	660	0.56	0	92.00	104.00	[34]
200	6.70	6.3	70	660	0.80	0	92.00	109.50	[34]
201	6.70	11.3	135	400	1.35	0	92.00	104.90	[34]
202	2.00	3	-	-	0	0	36.40	36.50	[35]
203	2.00	3	10	1803	1.40	0	36.40	102.80	[35]
204	2.00	3	20	1803	0.72	0	36.40	74.50	[35]
205	2.00	3	30	1803	0.48	0	36.40	59.70	[35]
206	2.00	3	40	1803	0.36	0	36.40	55.70	[35]
207	2.50	8	55	515	1.40	1.40	85.20	79.90	[36]
208	2.50	8	80	515	0.97	1.40	85.20	82.30	[36]
209	2.50	8	110	515	0.70	1.40	85.20	75.20	[36]
210	2.50	8	160	515	0.48	1.40	85.20	74.50	[36]
211	1.67	8	55	515	1.40	1.40	85.20	76.90	[36]
212	3.33	8	55	515	1.40	1.40	85.20	85.30	[36]
213	2.50	8	55	515	1.40	1.40	101.30	100.20	[36]
214	2.50	8	80	515	0.97	1.40	101.30	97.20	[36]
215	2.50	8	110	515	0.70	1.40	101.30	96.20	[36]
216	2.50	8	160	515	0.48	1.40	101.30	95.90	[36]
217	1.67	8	55	515	1.40	1.40	101.30	90.70	[36]
218	3.33	8	55	515	1.40	1.40	101.30	103.30	[36]
219	2.50	8	55	515	1.40	1.40	118.30	114.10	[36]
220	2.50	8	80	515	0.97	1.40	118.30	109.70	[36]
221	2.50	8	110	515	0.70	1.40	118.30	114.50	[36]
222	2.50	8	160	515	0.48	1.40	118.30	112.10	[36]
223	1.67	8	55	515	1.40	1.40	118.30	109.00	[36]
224	3.33	8	55	515	1.40	1.40	118.30	118.80	[36]
225	2.86	9.5	50	467	2.10	1.60	67.30	76.00	[37]
226	2.86	9.5	40	467	2.60	2.00	67.30	75.50	[37]
227	2.86	9.5	50	467	2.10	2.00	67.30	77.90	[37]
228	2.86	9.5	55	467	1.90	2.00	67.30	66.10	[37]
229	2.86	9.5	60	467	1.70	2.00	67.30	68.70	[37]

230	2.86	9.5	50	467	2.10	2.40	67.30	69.30	[37]
231	2.86	9.5	50	467	2.10	2.80	67.30	77.00	[37]

405